WELDING RESEARCH

SUPPLEMENT TO THE *WELDING JOURNAL*, AUGUST 2015
Sponsored by the American Welding Society and the Welding Research Council

New Brazing Recipe for Ductile Niobium-316L Stainless Steel Joints

A new method was developed for intermetallic-free ductile niobium-316L stainless steel transition joints for superconducting radio frequency cavities

BY A. KUMAR, P. GANESH, R. KAUL, B. K. SINDAL, K. YEDLE, V. K. BHATNAGAR, P. RAM SANKAR, M. K. SINGH, S. K. RAI, A. BOSE, R. SRIDHAR, S. C. JOSHI AND L. M. KUKREJA

ABSTRACT

This paper describes a new brazing recipe for making intermetallic-free and ductile niobium-316L stainless steel transition joints for application in superconducting radio frequency cavities. Brittle Fe-Nb intermetallic compounds have remained a matter of concern in niobium-stainless steel joints made with the global practice of vacuum brazing that uses pure copper as the filler metal. Important measures adopted to suppress brittle intermetallic formation include the use of nickel plating on mating stainless steel surface as a diffusion barrier and wettability enhancer, and lower temperature, titanium-free brazing filler metal BVAg8. The resultant joints were free of brittle intermetallic compounds, which translated into ductile fracture in tensile and shear tests. The brazed joints displayed tensile and shear strengths of 150–191 and 103–118 MPa, respectively. The joints demonstrated a required level of hermeticity for service in ultrahigh vacuum; a capability to withstand degassing heat treatment at 873 K, a mandatory step for superconducting radio frequency cavities; and also low-cycle thermal fatigue between the room temperature and the liquid nitrogen temperature. The new vacuum brazing recipe marks a significant advancement over existing global practice to make sound and ductile niobium-316L stainless steel transition joints with improved microstructural characteristics.

KEYWORDS

• Vacuum Brazing • Niobium • 316L Stainless Steel • BVAg8
• Diffusion Barrier • Superconducting RF Cavity

Introduction

Superconducting radiofrequency (SRF) cavities are key components of modern particle accelerator systems (Refs. 1, 2). Major benefits offered by SRF cavities include reduced power dissipation and possibility of operating with higher beam current. These SRF cavities, made of niobium, are submerged in a helium tank maintained at 2 K. At present, titanium is being widely used as the material of construction of the helium tank due to the proximity of its coefficient of expansion with niobium [$a_{Ti}/a_{Niobium}$ = 1.16 (Refs. 3, 4)]. There are serious attempts to replace titanium with AISI 316L stainless steel (SS) to make related fabrication processes simpler and cost effective (Refs. 5–9). However, construction of an austenitic SS helium tank of SRF cavities would necessitate a dissimilar transition joint between niobium and austenitic SS. This transition joint is not only required to display a high level of hermeticity in terms of helium leak tightness better than 1×10^{-10} mbar.lit/s at the room temperature (RT) as well as at 2 K for its operation in ultrahigh vacuum (UHV) environment, but should also withstand 10-h degassing heat treatment at 873 K (Ref. 10), and thermal cycling between RT and 2 K (Ref. 7). It may be noted that the heat treatment at 873 K is recommended for niobium cavities to drive out hydrogen contamination, introduced as a result of preceding mechanical and chemical treatments (Ref. 10). This dissolved hydrogen is responsible for Q-disease (represents severe degradation of the SRF cavities' quality factor) and the same must be removed in order to avoid formation of normal conducting niobium hydride on the niobium surface during the cool down of the cavity (Ref. 11). Major challenges involved in establishing sound niobium-316L SS transition joint include 1) large mismatch in coefficients of thermal expansion [$a_{Niobium}$: 6.9×10^{-6} K^{-1} (Ref. 12); a_{316SS}: 15.3×10^{-6} K^{-1} (Ref. 13)], and 2) strong tendency of niobium to form brittle intermetallic compounds with Fe in fusion welding (Ref. 14). Solid-state joining processes like hot isostatic pressing (HIP) (Ref. 15), explosion bonding (Ref. 16), and vacuum furnace brazing (Refs. 17–20) have been developed to establish satisfactory joining of these two metals to facilitate fabrication of 316L SS helium tanks for the SRF cavities.

Vacuum brazing, due to its versatility, ease, familiarity, and availability of technology in almost all particle accelerator laboratories, is the most attractive method for the above application.

A. KUMAR, P. GANESH, R. KAUL (rkaul@rrcat.gov.in), *B. K. SINDAL, K. YEDLE, V. K. BHATNAGAR, P. RAM SANKAR, M. K. SINGH, S. K. RAI, A. BOSE, R. SRIDHAR, S. C. JOSHI, AND L. M. KUKREJA are with Raja Ramanna Centre for Advanced Technology, Indore, India.*

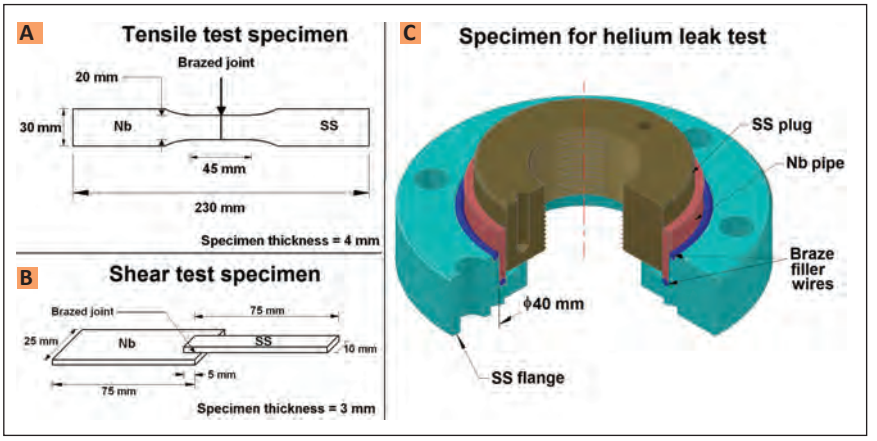

Fig. 1 — Details of vacuum-brazed niobium-316L stainless steel specimens used for the study.

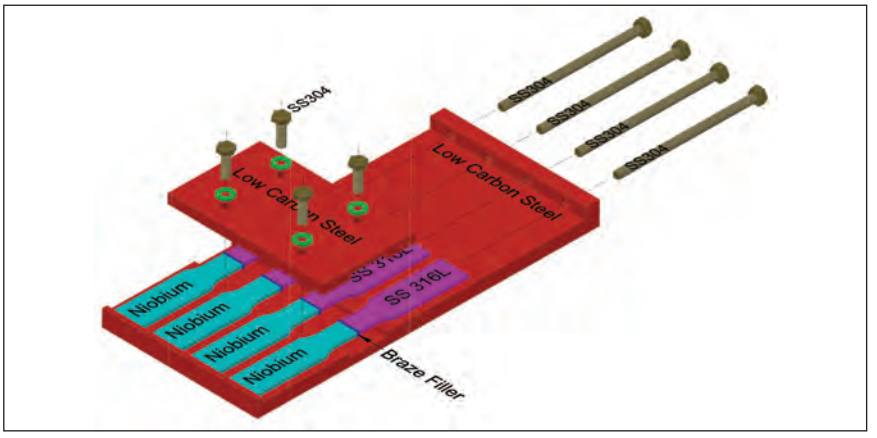

Fig. 2 — Exploded view of prebraze assembly of niobium and stainless steel parts in a specially made fixture for preparing tensile test specimens.

Fig. 3 — Helium leak testing of vacuum-brazed niobium-316L stainless steel specimen at room temperature.

In 1984, J. Susta of European Organization for Nuclear Research (CERN), Geneva, reported vacuum brazing of niobium to SS while using 80Au-20Cu as the brazing filler metal (BFM) (Ref. 17). The resultant brazed joints, although leak tight, were found to be unreliable when subjected to large forces. Poor mechanical properties of the brazed joint were attributed to a brittle intermetallic formation at the niobium/braze interface. In 1987, Bacher et al of CERN reported brazing of AISI 316LN SS to niobium using pure copper as the BFM (Ref. 18). The brazed joints, in spite of associated brittleness due to formation of Fe-rich compounds at the niobium/braze interface, satisfied all the criteria for their application in ultrahigh vacuum. It was suggested that during brazing Fe diffused across braze metal (pure copper) to form a layer of Fe-Nb intermetallic compound at the niobium/braze interface. CERN's vacuum brazing scheme was subsequently adopted by Argonne National Laboratory (ANL) to develop leak-tight and reliable niobium/SS brazed transition joints for use in the drift-tube SRF cavities of the Rare Isotope Accelerator (Ref. 19). The resultant transition joints were successfully operating on a prototype two-cell spoke cavity. On the basis of works reported by Bacher et al. (Ref. 18) and Fuerst et al. (Ref. 19), Ristori et al. proposed a modified joint design for joining an austenitic SS ring stiffener with its niobium counterpart (Ref. 7). In a recently reported experimental study performed in the authors' laboratory, a new lower temperature brazing scheme was adopted to obtain leak-tight, strong, and ductile niobium/austenitic SS brazed joints free of a brittle layer of Fe-Nb intermetallic compounds (Ref. 20).

The two-pronged approach, adopted to minimize formation of a brittle layer of Fe-Nb intermetallic compounds in the brazed joint, relied on good wettability of titanium-activated silver-based BFM (63Ag-35.25Cu-1.75Ti) of a lower melting range (1053–1088 K) and the use of nickel plating (on SS part) as a diffusion barrier. The resultant brazed joints not only exhibited required hermeticity (helium leak tightness better than 1×10^{-10} mbar.lit/s) for service in ultrahigh vacuum, but also withstood a 12-h degassing heat treatment at 873 K and 10 thermal cycles between RT and liquid nitrogen (LN_2) temperature, with no noticeable degradation in the microstructure and the hermeticity. The vacuum-brazed joints, made with titanium-activated silver-based BFM, displayed no brittle intermetallic layers on any of its interfaces, but instead carried well-distributed intermetallic particles in the ductile matrix. This resulted in improved joint ductility over that reported for joints made through existing global practice using pure copper as the BFM. The intermetallic particles were formed as a result of the reaction of Ti present in the BFM with Cu and Ni.

In subsequent efforts, directed at minimizing brittle intermetallic formation, some of the brazed specimens were made with BFM BVAg8 (72Ag-28Cu eutectic; T_M = 1053 K) of AWS specification A5.8 (Ref. 23). This BFM, with no titanium content, displayed good metallic bonding with both the substrates viz. niobium and Ni-plated 316L SS. The results were surprising

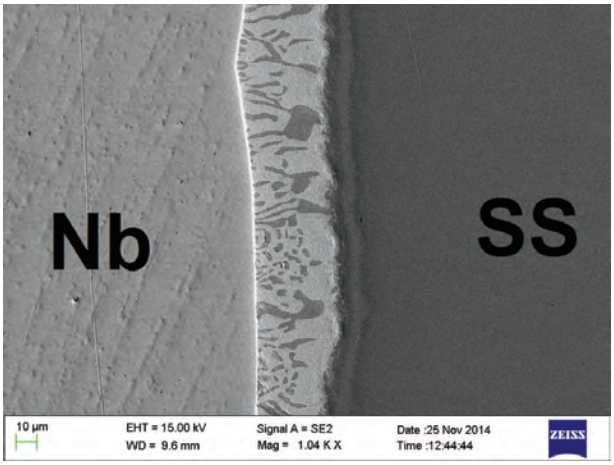

Fig. 4 — Cross section of niobium-316L stainless steel (SS) brazed specimen.

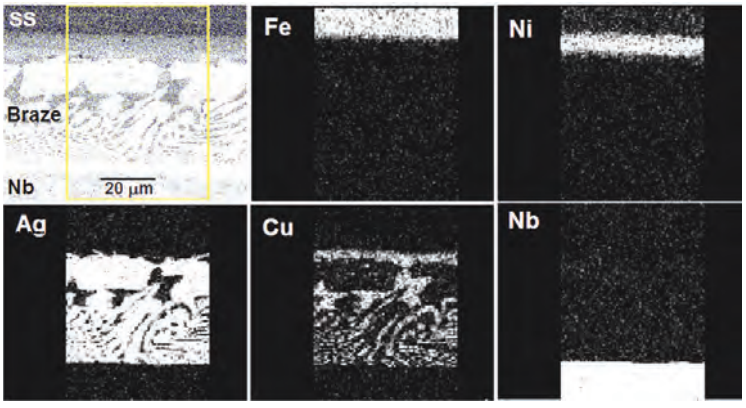

Fig. 5 — Secondary electron image and associated EDS concentration maps of Fe, Nb, Ni, Cu, and Ag across niobium-316L stainless steel (SS) brazed joint. The region used for EDS analysis is marked as a rectangle on secondary electron image.

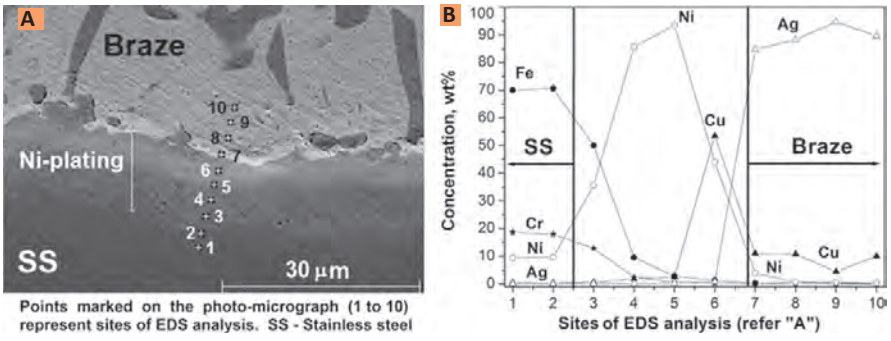

Fig. 6 — Secondary electron image and associated EDS concentration profiles of Fe, Cr, Ni, Cu, and Ag across Ni-plated 316L stainless steel (SS)/braze interface.

in view of a previously reported poor wettability of the niobium surface by this BFM (Ref. 22).

In light of the above finding, the present experimental study was taken up with an objective to further improve ductility of niobium-316L SS transition joints by completely eliminating brittle intermetallic formation. The approach, adopted to form sound intermetallic-free niobium-316L SS braze joints, included the use of vacuum-grade, titanium-free BVAg8 BFM, shorter time at brazing temperature, use of nickel plating as a diffusion barrier on SS part, improved surface cleanliness, and narrower joint clearance between mating surfaces. A similar approach has been reported for brazing Ti-6Al-4V and 17-4 PH SS (Refs. 23, 24).

To the best of our knowledge, the present work represents the first use of BVAg8 filler metal for making brazed joints involving niobium and nickel-plated austenitic SS.

Experimental Procedure

The procedure adopted for nickel electroplating on the SS part involved 1) ultrasonic cleaning in trichloroethylene for 20 min to remove oil, grease, and dust particles; 2) soak cleaning in alkaline solution of NaOH (20 g/L), Na_2CO_3 (20 g/L), and Na_3PO_4 (32 gm/L) for 20 min at 323–328 K; 3) chemical cleaning for 15–20 min in a solution of HNO_3, (20% v/v) and HF (2%) at RT followed by 1 min anodic and cathodic cleaning in H_2SO_4 (20% v/v) at a current density of 0.05 A/cm^2; 4) nickel strike in chloride nickel bath ($NiCl_2$ and HCl) for 5 min at a current density of 0.05 A/cm^2; 5) nickel deposition for 5 min in Watts' bath containing nickel sulfate, nickel chloride, and boric acid at a current density of 0.03 A/cm^2 at 323–328 K. The thickness of nickel plating was found to be 2–3 µm. On the other hand, the niobium specimens used for vacuum brazing were cleaned by buffer chemical polishing, involving immersion for 3 min in a solution of HF, HNO_3 and H_3PO_4 (in the ratio of 1:1:2).

Three sets of brazed specimens were prepared for the study, as shown in Fig. 1. The first set of brazed specimens was made in lap configuration between 3-mm-thick sheets of niobium and 316L SS, while sandwiching 50-µm-thick foil of BVAg8. These specimens were meant for conducting metallographic analysis and shear tests. The second set of brazed specimens was tensile test specimens made in butt configuration between two 4-mm-thick parts of niobium and 316L SS, while using 50-µm-thick foil of BFM. The tensile test specimens, with BFM sandwiched between mating faces of niobium and SS parts, were preassembled in a nickel-plated (15 mm) low-carbon steel fixture, as shown in Fig. 2. The choice of low-carbon steel as the material of construction of the fixture was based on its mean coefficient of thermal expansion between RT and 1073 K [15.4 ¥ 10^{-6} m/m.K (Ref. 3)] which falls between those of niobium [7.72 ¥ 10^{-6} m/m.K (Ref. 4)] and 316L SS [19.4 ¥ 10^{-6} m/m.K (Ref. 3)]. In order to keep the joint under compression at brazing temperature, the total expansion of niobium and SS parts should be matched by the expansion of the fixture during brazing. This requires the following equation to be satisfied:

$$a_{Nb}.L_{Nb}.DT + a_{SS}.L_{SS}.DT = a_{Fixture}.L_{Fixture}.DT \quad (1)$$

where, a_{Nb}, a_{SS}, and $a_{Fixture}$ represent

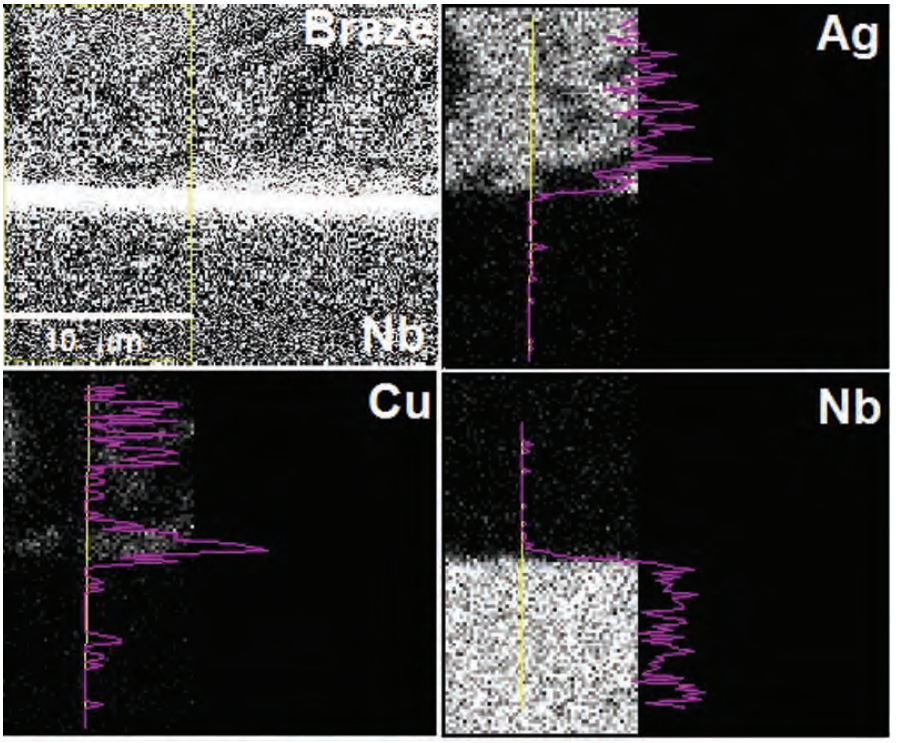

Fig. 7 — Secondary electron image and associated EDS concentration maps of Ag, Cu, and Nb across niobium/braze interface.

coefficients of thermal expansion of Nb part, SS part (inclusive of bolt — Fig. 2), and the fixture, respectively and L_{Nb}, L_{SS} and $L_{Fixture}$ represent lengths of Nb part, SS part (inclusive of bolt — Fig. 2), and the fixture, respectively.

By considering mean coefficients of thermal expansion of Nb, SS, and low-carbon steel (fixture material), Equation 1 yields $L_{Fixture} \approx 3L_{Nb} \approx 1.5L_{SS}$, which has been used for designing the fixture for brazing tensile test specimens.

During preassembly, a small prestress was applied to retain the BFM in place during the heatup. The nickel plating on the low-carbon steel fixture was meant to provide a diffusion barrier for the absorbed gases in the material. In order to study capillary brazing, a third specimen was prepared (Fig. 1C); it involved brazing of niobium pipe with 316L SS flange, 2¾ in. OD as per ASTM E2734/E2734M-10 (Ref. 25) with 1.6-mm-diameter BFM wires (Fig. 1). This brazed specimen was subsequently characterized by helium leak and other tests meant to determine the joint's hermeticity and its capability to withstand 10-h degassing heat treatment at 873 K and also service-induced thermal cycling between RT and 2 K. In the pipe/flange assembly, the measures adopted to ensure desired joint clearance at brazing temperature included tight dimensional tolerance of ±10 μm on the diameters of the mating surfaces of niobium pipe and SS flange, insertion of an austenitic 316L SS plug (precooled in LN_2) into niobium pipe, and shrink fitting of niobium pipe into SS flange. The approach of insertion of austenitic SS plug into niobium pipe for controlling the brazing joint clearance has also been adopted by CERN and ANL as well as by the authors in their recently reported experimental study (Ref. 20).

Brazing of the specimens was performed in an indigenously built hydrocarbon-free vacuum furnace at a pressure of 2×10^{-5} mbar. The job temperature was measured by inserting Inconel-sheathed N-type job thermocouples in thermowells provided in the brazing fixture of tensile test specimens and also in the sacrificial SS plug of the pipe-flange specimen in the close vicinity of the braze location. The depth of the thermowells was kept about 5 times its diameter, which was slightly more than the diameter of the sheathed thermocouple (3 mm) to facilitate its easy insertion. The thermal cycle used for niobium/316L SS brazing was RT; 523 K at 3 K/min, soaking at 523 K for 10 min; 523–823 K at 2 K/min, soaking at 823 K for 10 min; 823–1033 K at 3 K/min, soaking at 1033 K for 14 min; 1033–1073 K at 5 K/min, soaking at 1073 K for 1 min; followed by furnace cooling to RT. At the brazing temperature, the partial pressures of oxygen and water vapor were recorded as 2×10^{-9} mbar and 4×10^{-7} mbar, respectively. After brazing, the sacrificial SS plug was machined out before the brazed assembly was subjected to further testing. Simulated degassing heat treatment of the brazed assembly was carried out in the same vacuum furnace at 873 K. It may be noted that in contrast to authors' recently reported study, the brazed assembly was heat treated without taking any precautionary measures like inserting a removable SS plug into niobium pipe and tightly wrapping the outer surface of the SS flange with molybdenum wire (Ref. 20).

The brazed specimens were characterized with respect to 1) microstructure and compositional details of the brazed joint, 2) strength and fracture mode in tensile and shear tests, 3) hermeticity, and 4) their capability to withstand 10-h degassing heat treatment at 873 K and thermal cycling between RT and LN_2 temperature (77 K). The characterization techniques employed for microstructural and compositional analysis included scanning electron microscopy (SEM), energy-dispersive spectroscopy (EDS), and X-ray diffraction with CuKα characteristic radiation (λ = 1.54 Å). Helium leak rate measurements were performed on the vacuum-brazed tube/flange specimen (Fig. 1C) at RT as well as at LN_2 temperature. During helium leak testing (HLT) at RT, FKM (ASTM D1418-10a) O-rings and FKM sheets were used for sealing at SS flange and niobium pipe interfaces, respectively. For conducting HLT at LN_2 temperature, a 250-mm-long, thin adapter pipe, with one end welded to an ISO-KF 25 flange and the other end welded to a 316L SS type, 2¾-in.-OD flange (Ref. 25), was used to ensure temperature gradient from RT to LN_2 temperature in the pipe. The SS pipe was connected to the helium leak detector through a standard SS bellow using the ISO-KF

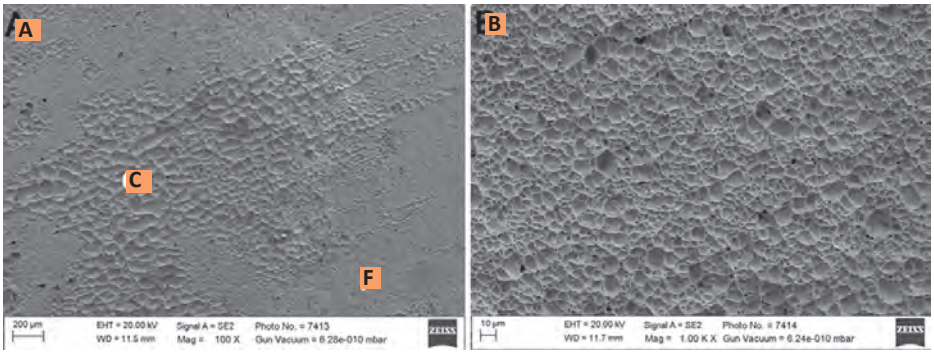

Fig. 8 — Fracture surface of tensile tested niobium-316L stainless steel brazed specimen. A — coarse and fine dimpled regions; B — magnified view of fine dimpled region — (C) coarse dimpled region, (F) fine dimpled region.

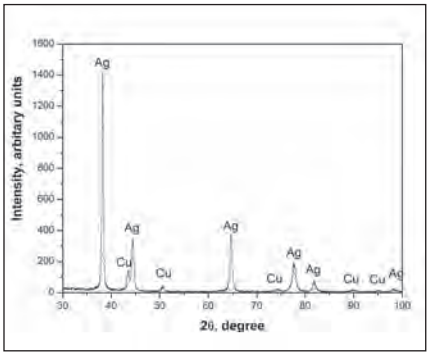

Fig. 9 — X-ray diffraction plots of mating fracture surfaces of tensile-tested niobium 316L stainless steel specimen.

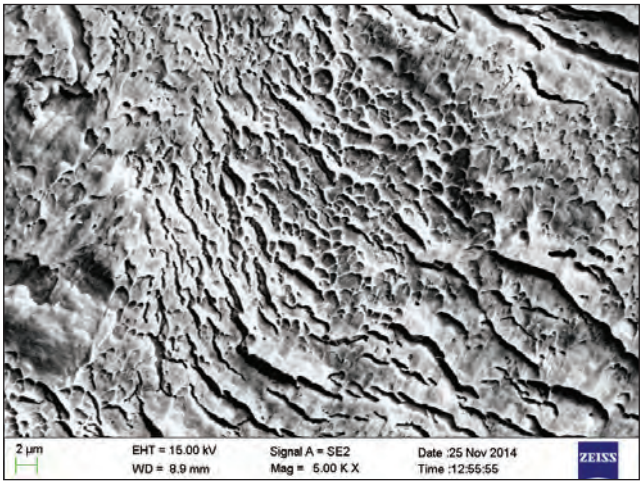

Fig. 10 — Magnified view of fracture surface of shear-tested niobium-316L stainless steel specimen.

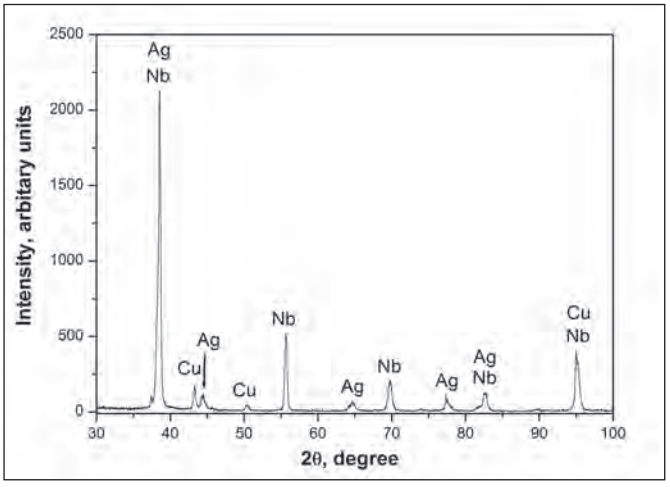

Fig. 11 — X-ray diffraction plots of fracture surface of shear tested niobium-316L stainless steel specimen.

25 interface and a FKM O-ring. The SS flange and the flat end face of niobium pipe of the brazed specimen were sealed with copper gasket and indium wire, respectively. During HLT, hermeticity of the brazed joint was determined by spraying helium from outside. Figure 3 presents helium leak testing of niobium pipe/SS flange specimen at RT. The thermal cycling test involved exposure of the brazed specimen to 10 thermal cycles between RT and the LN_2 temperature. It should be noted that most of the contraction of materials occurs between 300 and 77 K (Refs. 26–28). Hence, the thermal cycling test between 300 and 77 K (in place of 2K) gives a preliminary validation of reliability of niobium-316L SS brazed joints against service-induced low-cycle fatigue conditions. After each thermal cycle, the brazed joint's integrity was determined by subjecting it to HLT.

Results

Metallographic examination of transverse cross section of vacuum-brazed specimens, made between niobium and nickel-plated 316L SS sheets in lap configuration, revealed sound brazed joints, as shown in Fig. 4. The joint did not exhibit any distinct layer on either of its two interfaces, viz. niobium/braze and SS/braze. There was no intergranular penetration of BFM into SS part (Ref. 29). The joint displayed two-phase microstructure, with Ag-rich bright and Cu-rich dark phases. It is to be noted that nickel, diffused out of the electroplated layer, was predominantly present in the Cu-rich dark phase of the brazed joint. The brazed joint was characterized by a sharp niobium/braze interface due to limited solubility of niobium in Ag and Cu and vice versa. On the other hand, SS/braze interface, due to unlimited mutual solubility of copper and nickel, was diffused in nature.

The average chemical composition (in wt-%) of the brazed joint, as determined by EDS, was Ag = 68.23, Cu = 29, and Ni = 2.77. Figure 5 presents mapping of various elements, as determined by EDS, across the transverse cross section of the brazed joint. The brazed joint displayed no noticeable enrichment of any alloying element on either of its interfaces viz. niobium/braze and SS/braze.

The well-bonded nickel electroplated layer on the surface of SS part remained intact after brazing. The electroplated layer displayed dilution from Cu (from the brazing filler), Fe and Cr (from SS part), beside some diffusion of Ni into SS part. Figure 6 presents SEM photomicrograph and associated EDS profile across SS/braze interface. Detailed EDS analysis of the niobium/ braze interface at a higher magnification did not

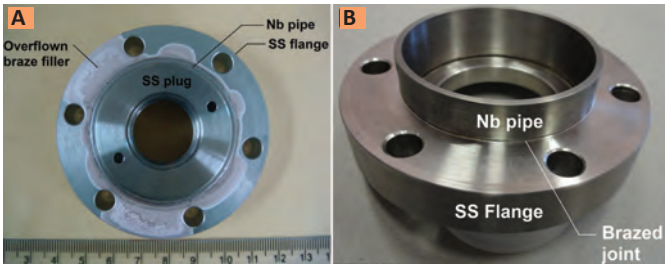

Fig. 12 — Vacuum brazed niobium pipe/316L stainless steel flange specimen. A — in as-brazed condition; B — after machining. Note significant spread of braze filler on the surface of Ni-plated SS flange.

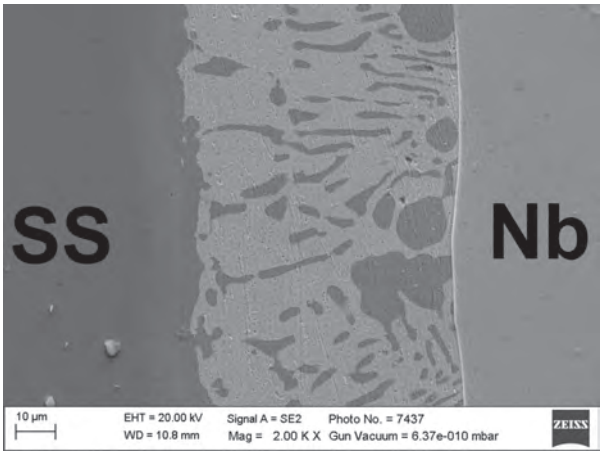

Fig. 13 — Cross section of vacuum-brazed niobium-316L stainless steel (SS) specimen heat treated at 873 K.

bring out any noticeable mutual diffusion of niobium and Ag as well as niobium and Cu, as shown in Fig. 7.

Tensile testing of three numbers of vacuum-brazed niobium/316L SS specimens displayed joint strength of 150, 188, and 191 MPa, respectively. The site of fracture remained in the braze metal. Tensile fracture of the brazed specimens in the braze metal suggests absence of any brittleness at either of the two interfaces (viz. niobium/braze and SS/braze). Detailed examination of resultant fracture surfaces revealed a dimpled fracture surface representing a ductile mode of fracture. The fracture surface exhibited mixed distribution of coarse and fine dimples, as shown in Fig. 8. Average chemical composition (in wt-%) of the fracture surface (niobium side of the fractured specimen) was Ag = 77.86, Cu = 18.3, Ni = 2.41, and Nb = 1.43 with no presence of Fe. It was confirmed that the presence of niobium on the fracture surface was attributed to localized pinhole porosity in the braze layer, which served to expose underneath niobium. Fracture surfaces of tensile-tested brazed specimens were analyzed by X-ray diffraction to determine various phases formed in the braze joint. The results exhibited the presence of silver and copper on tensile fracture surface. Figure 9 presents X-ray diffraction plot of the fracture surface of tensile tested niobium-316L SS specimen.

On the other hand, shear testing of two numbers of brazed specimens exhibited joint strength of 103 and 118 MPa, with site of failure again falling in the braze metal. Detailed fractographic examination of sheared fracture surface revealed presence of fine elongated dimples representing the ductile mode of shear fracture. Figure 10 presents a scanning electron photo micrograph showing elongated dimples on sheared fracture surface of brazed niobium-316L SS specimen. X-ray diffraction of sheared fracture surface of niobium/316L SS brazed specimens exhibited presence of Ag and Cu, beside some niobium. Figure 11 presents an X-ray diffraction plot of sheared fracture surface of the niobium-316L SS specimen.

Figure 12 presents photographs of a vacuum-brazed niobium pipe/SS flange specimen (A) in as-brazed and (B) machined conditions. The top surface of the SS flange was unintentionally Ni plated because the surface was not masked during the Ni plating. It was found that the bottom BFM wire was consumed in brazing in spite of being completely concealed from radiative heating, but the top wire, which was exposed to radiative heat, displayed preferential spread on the nickel-plated top surface of the SS flange — Fig. 12A. This indicates that nickel plating should be restricted to the SS surface to be brazed for guided flow of molten BFM into the capillary clearance. Helium leak testing of vacuum-brazed pipe/flange assembly (after machining of sacrificial SS plug) at RT displayed helium leak tightness better than $1.0 ¥ 10^{-10}$ mbar.lit/s, thereby demonstrating suitability of the joint for service in ultrahigh vacuum environment. The braze specimen successfully withstood 10-h heat treatment at 873 K without experiencing any degradation in its hermeticity.

Metallographic examination of niobium-316L SS brazed joint after its exposure to ten-hour heat treatment at 873 K did not bring out any noticeable change in the microstructure, except further dissolution of the Ni layer into Cu-rich phase of the braze metal. Figure 13 presents a magnified view of the cross section of niobium-316L SS brazed joint. Like the as-brazed specimen, the heat-treated specimen also did not display any distinct layer on any of the brazed interfaces. Figure 14 presents mapping of various elements, as determined by EDS, across the transverse cross section of the brazed joint heat treated at 873 K. The heat treated brazed specimen was not found to be associated with any iron, chromium, or nickel migration toward the niobium interface; and intergranular penetration of BFM into the SS part.

Discussion

One of the important characteristics affecting the joining of refractory metals is their poor oxidation resistance, even at relatively low temperatures (Ref. 30). Niobium, like other refractory metals, is considered difficult to braze as it quickly develops adherent oxides when exposed to atmosphere at RT (Ref. 31). Surface oxide removal is mandatory before brazing of refractory metals, and the cleaning operation should be performed immediately before brazing to prevent contamination (Refs. 32, 33). It was recommended that the cleaned components must be preserved and protected from contamination for successful brazing of refractory metals (Ref. 34). In an experimental study performed by Liaw et al., it was demonstrated that the niobium surface, ultrasonically cleaned followed by an acetone

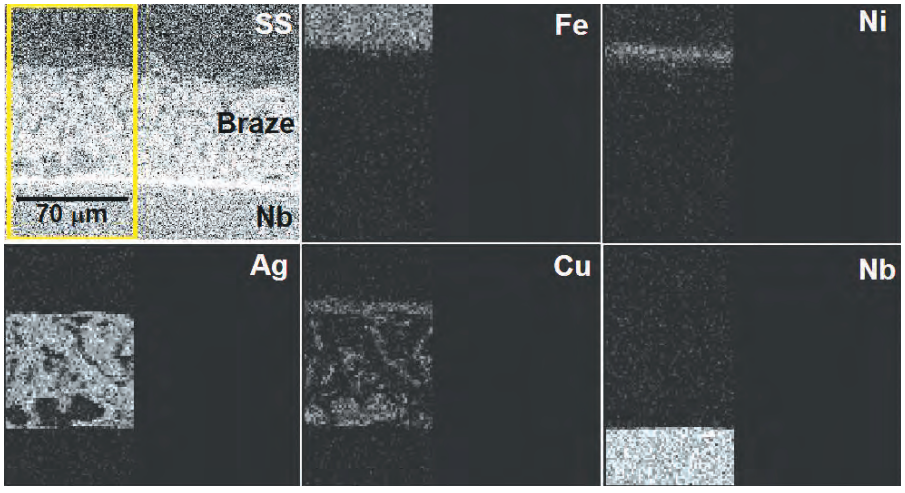

Fig. 14 — Secondary electron image and associated EDS concentration maps of Fe, Nb, Ni, Cu, and Ag across Nb-316L stainless steel (SS) brazed joint heat treated at 873 K. The region used for EDS analysis is marked as a rectangle on the secondary electron image.

swab, cannot be wetted by BAg8 BFM (72Ag-28Cu eutectic; T_M = 1053 K) in vacuum of 10^{-5} mbar (Ref. 21). Susta et al. observed that a good preparation of the base metal specimens is essential for successful brazing of niobium with SS (Ref. 17). The prebraze cleaning procedure adopted by various authors included cleaning with acetone followed by chemical cleaning (Refs. 7, 17). In this regard, simplified sessile drop measurements were performed to evaluate the wettability of buffer chemically polished niobium and ultrasonically cleaned Ni-plated SS substrates by BVAg8. In the experiment, a BVAg8 wire piece of 1.6 mm diameter and 4 mm height was placed vertically on each of the substrates and subjected to experimental brazing thermal cycle (within 1 h of surface cleaning). After cooling down to RT, the specimens were examined for contact angle measurement. The results of the substudy demonstrated that wettability of the buffer chemically polished niobium surface by BVAg8 remains poor (contact angle $\theta_{Niobium}$ ~ 160 deg), in contrast to excellent wettability of the Ni-plated SS surface (contact angle θ_{SS316L} ~ 0 deg).

Capillary brazing is even more sensitive to wettability of the surface as compared to sandwich brazing (Ref. 35). Poor wettability of niobium surface for BVAg8 does not explain the formation of sound braze joints in sandwich as well as capillary configuration. It may be noted that in the present case, the brazed joint was made between two dissimilar surfaces (niobium and Ni-plated SS), with widely different wetting characteristics. In contrast to niobium, the Ni-plated SS surface is known for its excellent wettability for BVAg8 (Ref. 36), which was also confirmed by the wettability experiment. In this type of joint, wetting of both the surfaces by the molten BFM must be taken into account. The criterion for spontaneous ingress of BFM into the capillary is $\theta_{niobium} + \theta 3_{16L} < 180$ deg (Ref. 35). Therefore, it can be inferred that poor wettability of the niobium surface was adequately compensated by excellent wettability of the Ni-plated SS surface, thereby facilitating spontaneous ingress of brazing filler metal BVAg8 into the capillary joint clearance. Extremely limited solubility of niobium in Ag and Cu and vice versa (Ref. 37) also helped in free flow of BVAg8 over the niobium interface due to little change in its eutectic composition (Ref. 38).

Distinct features of the vacuum-brazed niobium-316L SS joint were the absence of any distinct layer on either of its two interfaces, and the absence of intergranular penetration of BFM into SS part. Compositional mapping of the brazed joint did not bring out any noticeable presence of Fe, Cr, or Ni as reported in niobium-SS brazed joints made with pure copper as the BFM on the niobium/ braze interface (Refs. 18, 19). Distinct presence of the electroplated nickel layer (with some dilution from Cu and SS) on the SS/braze interface is indicative of the fact that the nickel layer did play its intended role as a diffusion barrier against migration of Fe toward niobium during brazing, while preventing intergranular penetration of Cu into the SS part. In addition, nickel plating also served to enhance wettability of BVAg8 on the SS surface.

Sharp niobium/braze interface is suggestive of little mutual diffusion across the interface. It may be noted that the Nb-Cu binary system displays little mutual solubility [Nb in Cu (at 293–1073 K) = 0.14–0.15 at.-%; Cu in niobium (at 1073–1273 K) = 0.6–0.7 at.-%] with respect to practically no mutual solubility for Nb-Ag binary system (Ref. 37). In view of the very limited mutual solubility of these two elements [falling well below the practical detectability limit of EDS (~ 1 at.-%)], coupled with ~ 1 μm lateral spread of the region yielding the X-ray signal, it is extremely difficult to comment on the extent of mutual diffusion of copper and niobium across the niobium/braze interface.

The formation of an integrally bonded brazed joint is controlled by solid solubility relationship between the BFM and the base metals. This requires diffusion of base metal into BFM or vice versa, even to the extent of a few atomic layers from the interface (Ref. 39). It is believed that despite limited mutual solid solubility of copper and niobium across the niobium/braze interface, a few atomic layers of interdiffusion of niobium and copper would have taken place to establish bonding between niobium and the braze metal. Ten-hour exposure of the brazed specimen to degassing heat treatment at 873 K did not introduce any noticeable degradation in the joint's microstructure. Failure of both tensile and shear-tested specimens exhibited dimpled fracture surfaces (with no signature of brittle intermetallic compounds), representing ductile fracture. It may be noted that ductile fracture occurs through formation of microvoids whose growth and subsequent coalescence gives a dimpled appearance to the resultant fracture surface. The process of microvoid growth involves considerable localized plastic deformation and requires the expenditure of large amounts of energy (Ref. 40). Coarser dimples, therefore, signify a greater degree of plastic deformation before microvoids coalesce to bring about fracture. Relatively higher ductili-

ty of the Ag-rich phase over the Cu-rich phase is responsible for mixed distribution of dimples on the resultant fracture surface. Absence of Ti in the BVAg8 (as compared to titanium-activated silver-based BFM) contributed to the elimination of brittle intermetallic compounds, thereby enhancing joint ductility.

Improved ductility of the brazed joint was largely responsible for the fact that the joint retained its hermeticity even after undergoing 10-h degassing heat treatment at 873 K and 10 thermal cycles between RT and LN_2 temperature. The results not only established suitability of the vacuum-brazed niobium-316L SS for operation in ultrahigh vacuum environments but also its capability to withstand subsequent processing and service-induced low-cycle fatigue conditions imposed by thermal cycling between RT and 2 K. However, for producing sound brazed joints, the nickel plating on the SS part needs to be strictly confined to the site of brazing so that uncontrolled spread of BFM (Fig. 12A) is avoided and sufficient braze metal is available to fill the capillary clearance.

Conclusions

The results of the present investigation have demonstrated that vacuum brazing of niobium to nickel-plated austenitic SS with BVAg8 resulted in a sound transition joint without brittle intermetallic formation in spite of its reportedly poor wettability on niobium surface. Development of a vaccuum-brazed joint, free of brittle intermetallic compounds, not only marked significant improvement over existing global vacuum brazing practice that uses pure copper as the filler metal, but also over the authors' own recently reported results with titanium-activated silver-based BFM where the brazed joint displayed well-distributed intermetallic compounds in the ductile phase. Vacuum-brazed specimens displayed helium leak tightness better than $1 ¥ 10^{-10}$ mbar.lit/s and also withstood 10-h degassing heat treatment at 873 K and 10 thermal cycles between 300 and 77 K without any degradation in the joint's hermeticity; thereby establishing its suitability to withstand service-induced low-cycle fatigue conditions. Important contributing factors for establishment of a sound and ductile niobium-316L SS transition joint were 1) use of BVAg8 BFM, 2) use of nickel-plating as a diffusion barrier to suppress iron migration from SS part toward niobium, and 3) excellent wettability of nickel-plated SS surface, which compensated for poor wettability of the niobium surface. On the basis of the results of the study, a new lower temperature brazing route is proposed to make niobium-316L SS transition joints with improved microstructure and ductility for application in SRF cavities.

Acknowledgments

Authors are thankful to Dr. P. D. Gupta, Director, Raja Ramanna Centre for Advanced Technology, for encouraging indigenous technological developments. They wish to thank Mr. Avinash Puntambekar for many useful discussions for maintaining a direct linkage to the application of developed brazing recipe in the low beta SRF cavity. Authors thankfully acknowledge UGC-DAE-CSR, Indore and Corporate R & D, Bharat Heavy Electricals Ltd., Hyderabad, for providing SEM-EDS facility for characterization of the specimens. They express their sincere thanks to Mr. V. K. Ahire of UGC-DAE-CSR for EDS analysis of the specimens. Authors thank Mr. A. P. Singh, Mr. C. Manikandan, and Mr. G. S. Deshmukh for their useful contribution in chemical cleaning and nickel electroplating. They thankfully acknowledge technical assistance of Mr. R. Chouhan, Mr. S. K. Chourasia, Mr. J. S. Pulickal, Mr. Vedpal, Mr. Om Prakash, Mr. S. Sarkar, Mr. N. More, Mr. T. R. Meena, Mr. D. C. Nagpure, and Mr. Ram Nihal Ram during various stages of the investigation. Authors also thank Mr. J. D. Zolpara and Mr. B. Oraon for preparing drawings of test specimens and fixtures.

References

1. Jana, A. R., Kumar, V., Kumar, A., and Gaur, R. 2013. Electromagnetic design of a 650-MHz superconducting radio frequency cavity. *IEEE Transactions of Applied Superconductivity* 23(4): 3500816.

2. Nema, P. K. 2011. Application of accelerators for nuclear systems: Accelerator driven system (ADS). *Energy Procedia* 7: 597–608.

3. *ASME Boiler and Pressure Vessel Code*, Section II-Part D, 2010 edition, pp. 725,708,711.

4. *ASM Handbook*. 1979. 9th ed., Vol. 2, p. 778, Ohio: ASM International.

5. Brandt, J., Barbanotti, S., Wands, R., Dhanaraj, N., Khabiboulline, T., Carter, H., Foley, M., and Grimm, C. 2010. SS helium tank development for 1.3 GHz SRF cavity at Fermilab, *Proc. Linear Accelerator Conf. LINAC2010*, pp. 596–598.

6. Atieh, S., Izquierdo, G. A., Aviles, S. I., Capatina, O., Renaglia, T., Tardy, T., Valverde A. N., and Weingarten, W. 2011. Mechanical design and fabrication studies for SPL superconducting RF cavities. *Proc. International Particle Accelerator Conf. IPAC-2011*. pp. 199–201.

7. Ristori L., and Toter, W. 2012. Development at ANL of a copper brazed joint for the coupling of the niobium cavity end wall to the stainless steel helium tank in the fermi lab SSR1 resonator. *Proc. International. Particle Accelerator Conf. IPAC-2012*, pp. 2345–2347.

8. Capatina, O., Atieh, S., Santillana, I. A., Izquierdo, G. A., Bonomi, R., Calatroni, S., Chambrillon, J., Gerigk, F., Garoby, R., Guinchard, M., Junginger, T., Malabaila, M., Ferreira, L. M. A., Mikulas, S., Parma, V., Pillon, F., Renaglia, T., Schirm, K., Tardy, T., Therasse, M., Vacca, A., Alonso N. V., and Craen, A. V. 2013. CERN developments for 704 MHz superconducting cavities. *Proc. International Conf. on RF Superconductivity, 2013*, pp. 1192–1205.

9. Saugnac, H., Rousselot, S., Commeaux, C., Gassot, H., Junquera, T., Bosland, P., and Safa, H. 2001. Preliminary design of stainless steel helium tank and its associated cold tuning system for 700 MHz SCRF cavities for proton. *Proc. Workshop on RF Superconductivity SRF-2001*, pp. 540–542.

10. Xie, Y. 2013. Development of superconducting RF sample host cavities and study of pit induced cavity quench, Ph.D. dissertation. Cornell University.

11. Bonin B., and Röth, R. W. 1991. Q-Degradation of niobium cavities due to hydrogen contamination. *Proc. Workshop on RF Superconductivity SRF-1991*, pp. 210–244.

12. *Smithells Metals Reference Book*. 2000. Edited by E. A. Brandes and G. B. Brook, 14.3–14.5, Oxford, UK: Butterworth-Heinemann.

13. Rouby, M., and Blanchard, P. in: P. Lacombe, B. Baroux, G. Beranger (Eds.). *Stainless Steels, Les Editions de Physique Les Ulis*, Cedex A, France, 1993, p. 139.

14. Kuchnir M., and Hiller, R. E. 1993. Welding of niobium to stainless steel, FERMILAB-TM-1831, Fermi National Accelera-

tor Laboratory, Batavia, Ill. *http://lss.fnal.gov/archive/test-tm/1000/fermilab-tm-1831.pdf*, visited on Sept. 4, 2014.

15. Saito, K., Inoue, H., Ao, H., and Satoh, N. 2001. Stainless steel flange bonded to niobium tube and simple aluminum sealing. *Proc. Workshop on RF Superconductivity*, pp. 531–533.

16. Sabirov, B., Budagov, J., Sissakian, A., Shirkov, G., Taran, Y., Trubnikov, G., Dhanarai, N., Foley, M., Harms, E., Klebaner, A., Mitchell, D., Nagaitsev, S., Soyars, W., Rybakov, V., Samarokov, Y., Zhigalov, V., Basti, A., and Bedeschi, F. 2011. Recent advances in Ti and niobium explosion welding with stainless steel for 2K operating (ILC Program). *Proc. International Workshop on Future Linear Colliders, 2011*, ID 440.

17. Susta, J., 1984. Development in fabrication methods. *Proc. SRF workshop*, pp. 597–610.

18. Bacher, J. P., Chiaveri, E., and Trincat, B. 1987. Brazing of niobium to stainless steel for UHV applications in superconducting cavities, CERN/EF/RF 87-7, CERN, Geneva, Switzerland. *http://cds.cern. ch/record /948207/files/CM-P00058114. pdf*, visited on Dec. 23, 2014.

19. Fuerst, J. D., Toter W. F., and Shepard, K. W. 2003. Niobium to stainless steel braze transition development, Proc. Workshop on RF-Superconductivity, pp. 305–307.

20. Kumar, A., Ganesh, P., Kaul, R., Bhatnagar, V. K., Yedle, K., Sankar, P. R., Sindal, B. K., Kumar, K. V. A. N. P. S., Singh, M. K., Rai, S. K., Bose, A., Veerbhadraiah, T., Ramteke, S., Sridhar, R., Mundra, G., Joshi, S. C., and Kukreja, L. M. 2014. A new vacuum brazing route for niobium-316L stainless steel transition joints for superconducting RF cavities. *Journal of Materials Engineering and Performance*, Available Online since 21st November, 2014, DOI: 10.1007/s11665-014-1312-1.

21. Liaw, D. W., and Shiue, R. K. 2005. Brazing of Ti-6Al-4V and niobium using three silver-base braze alloys. *Metallurgical and Materials Transactions* 36A: 2415–2427.

22. AWS A5.8M/A5.8:2011-AMD1. 2013. *Specification for Filler Metals for Brazing and Braze Welding*, 10th edition, American Welding Society.

23. Shiue, R. K., Wu, S. K., Chan, C. H., and Huang, C. S. 2006. Infrared brazing of Ti-6Al-4V and 17-4 PH stainless steel with a nickel barrier layer. *Metallurgical and Materials Transactions* A, 37(7), 2207–2217.

24. *https://app.aws.org/associations /bsmc/WJ_2013_02_brazingQnA.pdf*, visited on April 6, 2015.

25. ASTM E2734/E2734M-10. 2010. *Standard Specification for Dimensions of Knife-Edge Flanges*, ASTM International, West Conshohocken, Pa.

26. Poggiani, R. 2009. *Materials and Components of Possible Interest for Cryogenic Operation of Einstein Telescope*, ET-026-09, Issue 1, University of Pisa and INFN Pisa.

27. Marquardt, E. D., Le, J. P., and Redebaugh, R. 2000. Cryogenic Material Properties Database. *Proc. International Cryocoller Conf., http://www.cryogenics.nist.gov/Papers/Cryo_Materials.pdf*, visited on Jan 30, 2015.

28. Low temperature properties of materials. 2010. USPAS Cryogenics Short Course, Boston. *http://uspas. fnal.gov/materials/10MIT/Lecture_1.2.pdf*, visited on Dec. 23, 2014.

29. Heiple, C., Bennett, W., and Rising, T. 1982. Embrittlement of several stainless steels by liquid copper and liquid braze alloys. *Materials Science and Engineering* 52: 277–89.

30. *Brazing and Bonding of Columbium, Molybdenum, Tantalum, Tungsten and Graphite*, Report No. 278193, 1962, Defense Metals Information Center, Battelle Memorial Institute, Columbus, Ohio.

31. Palmer, A. J., and Woolstenhulm, C. J. 2009. Brazing refractory metals used in high-temperature nuclear instrumentation. *International. Conf. ANIMMA*.

32. Schwartz, M. 2003. *Brazing*, p. 305, Ohio: ASM International.

33. Boughton, J. D., and Roberts, P. M. 1973. Furnace brazing: A survey of modern processes and plant, Johnson Matthey Metals Limited, *http://www. jm-metaljoining.com/pdfs-uploaded/Furnace%20Brazing.pdf*, visited on Dec. 15, 2014.

34. *Welding Handbook*. 1992. 8th ed., Vol. 2. p. 409, Miami, Fla.: American Welding Society.

35. *Advances in Brazing — Science, Technology, and Applications*. 2013. Edited by D. P. Sekulić, 3-28, Philadelphia, Woodhead Publishing Ltd.

36. Hosking, F. M., Stephens, J. J., and Rejent, J. A. 1999. Intermediate temperature joining of dissimilar metals. *Welding Journal* 78(4): 127-s to 136-s.

37. Shabalin, I. L. 2014. *Ultra-High Temperature Materials I: Carbon (Graphene/Graphite) and Refractory Metals*. p. 558, New York, Springer Dordrecht Heidelberg.

38. Sloboda, M. H. 1961. *Design and Strength of Brazed Joints*. p. 5, London: Johnson Matthey & Co Limited.

39. Tweeddale, J. G. 2013. The fabrication of materials. *Materials Technology*. p. 129, London: Elsevier.

40. Davis, J. R. 1998. *Metals Handbook*–Desk Edition. 1214, Ohio: ASM International.